

Oral Bioavailability, Tissue Distribution, Metabolism, and Excretion of Panduratin A from *Boesenbergia rotunda* Extract in Healthy Rats

Teetap Kongratanapasert^{1,2}, Tussapon Boonyarattanasoonthorn³, Kittitach Supannapan⁴, Suradej Hongeng⁵, Phisit Khemawoot¹

¹Chakri Naruebodindra Medical Institute, Faculty of Medicine Ramathibodi Hospital, Mahidol University, Samutprakarn, Thailand; ²Program in Translational Medicine, Faculty of Medicine Ramathibodi Hospital, Mahidol University, Bangkok, Thailand; ³Chulalongkorn University Laboratory Animal Center, Chulalongkorn University, Bangkok, Thailand; ⁴Chao Phraya Abhaibhubejhr Hospital Foundation, Prachinburi, Thailand; ⁵Department of Pediatrics, Faculty of Medicine Ramathibodi Hospital, Mahidol University, Bangkok, Thailand

Correspondence: Phisit Khemawoot, Chakri Naruebodindra Medical Institute, Faculty of Medicine Ramathibodi Hospital, Mahidol University, Tel/Fax +66 28395161, Email phisit.khe@mahidol.ac.th

Background: Our previous studies in vitro and in vivo have shown anti-severe acute respiratory syndrome coronavirus 2 activity of fingerroot extract (*Boesenbergia rotunda*) and its phytochemical panduratin A.

Aim of Study: Therefore, the objective of this study was to determine the pharmacokinetic profiles of panduratin A, as a pure compound and in fingerroot extract, in rats.

Materials and Methods: Male rats were randomly divided into four groups. Rats underwent intravenous administration of 4.5 mg/kg panduratin A, a single oral administration of 45 mg/kg panduratin A, or a multiple oral administration of 45 mg/kg panduratin A-consisted fingerroot extract for 7 consecutive days. The concentrations of panduratin A in plasma, tissues, and excreta were measured by using LCMS with a validated method.

Results: The rats showed no change in health status after receiving all test preparations. The absolute oral bioavailability of panduratin A administered as pure panduratin A and fingerroot extract were approximately 9% and 6%, respectively. The peak concentrations for the single oral doses of 45 mg/kg panduratin A and fingerroot extract, were 4833 ± 659 and 3269 ± 819 $\mu\text{g/L}$, respectively. Panduratin A was mostly distributed in gastrointestinal organs, with the highest tissue-to-plasma ratio in the stomach. Approximately 20–30% of unchanged panduratin A from the administered dose was detected in feces while a negligible amount was found in urine. The major metabolites of administered panduratin A were identified in feces as oxidation and dioxidation products.

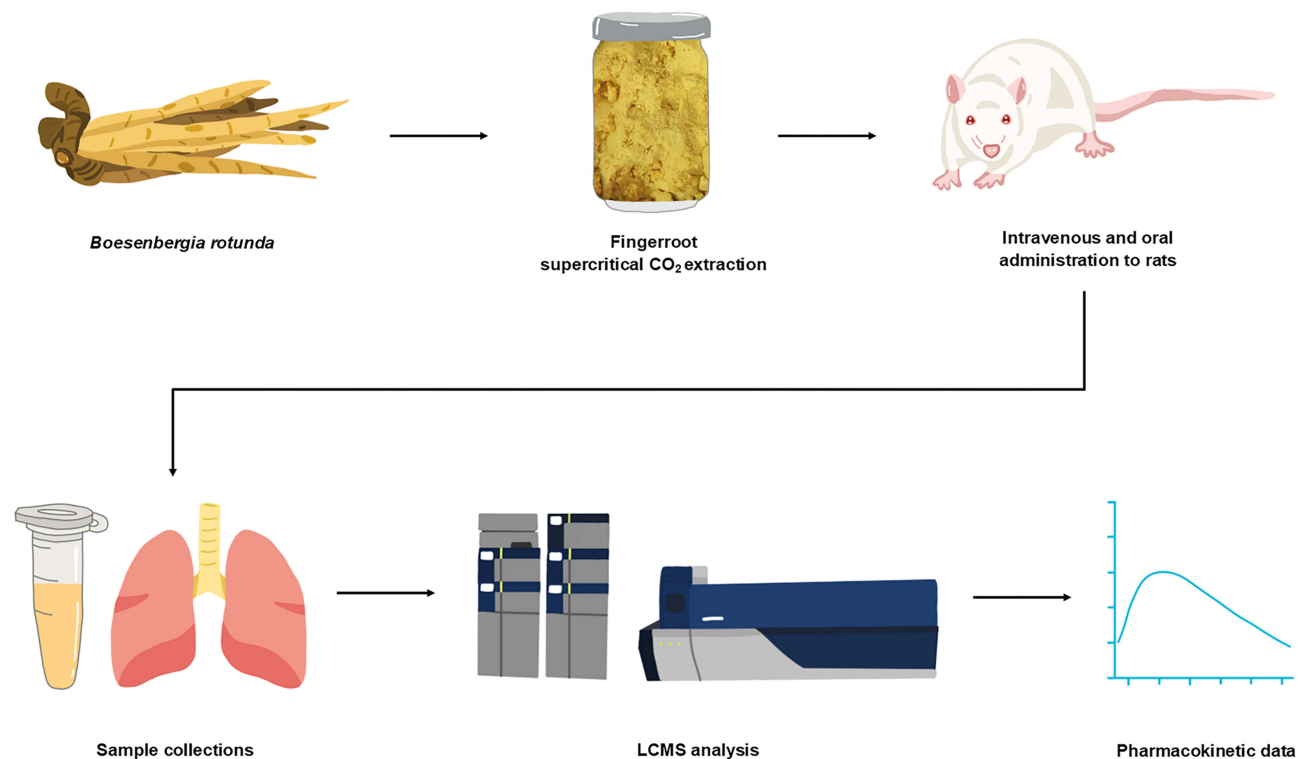
Conclusion: Panduratin A from fingerroot extract showed low oral bioavailability, good tissue distribution, and partially biotransformed before excretion via feces. These findings will assist in developing fingerroot extract as a phytopharmaceutical product for COVID-19 treatment.

Keywords: pharmacokinetics, tissue distribution, biotransformation, panduratin A, *Boesenbergia rotunda*, COVID-19

Introduction

In 2020, the world was faced with the event with the greatest impact in modern history, the outbreak of Coronavirus disease 2019 (COVID-19) caused by severe acute respiratory syndrome coronavirus 2 (SARS-CoV-2).^{1,2} Even though in 2023 vaccines and medications are available, infection and death are still occurring.^{3,4} The utilization of herbal products has been deemed a viable strategy for confronting the challenges of emerging and re-emerging diseases.^{5,6} In our previous study, the 122 extracts from Thai medicinal plants and their active compounds that were screened for anti-SARS-CoV-2 activity in Vero E6 cells, fingerroot extract, and its active constituent, panduratin A, demonstrated anti-SARS-CoV-2 activity with IC_{50} values of 3.62 $\mu\text{g/mL}$ and 0.81 μM , respectively, compared to that of remdesivir, with an IC_{50} of 2.71 μM .⁷ However, fingerroot extract was used rather than pure panduratin A because of the limitations and cost

Graphical Abstract



of the purification process. We then verified the efficacy of an ethanol extract of fingerroot in SARS-CoV-2-infected hamsters. Administration of 300–1000 mg/kg/day of ethanolic fingerroot extract for 7 days reduced lung inflammation and cytokine levels.⁸

Boesenbergia rotunda (L.) Mansf. (Zingiberaceae), or fingerroot is a plant used in local food and traditional medicine located in Southern China, Southeast Asia, and South Asia.⁹ Fingerroot has been shown to exhibit antibacterial, anti-inflammatory, antioxidant, anticancer, and nephroprotective effects.^{10–15} Fingerroot extract showed activities against pathogenic bacteria (*Listeria monocytogenes*, *Bacillus cereus*, and *Staphylococcus aureus*) with an MIC value of 0.2–0.4% (v/v).¹⁶ Moreover, the plasma level of the cytokine interleukin-6 in ulcer rats was reduced by fingerroot.¹⁷ Panduratin A, the major bioactive substance of fingerroot, contains physicochemical properties with the ability to donate two and accept four hydrogen bonds, and it has a molecular weight of 406.5 g and an XlogP value of 7.08.¹⁸ In terms of efficacy, panduratin A was reported to inhibited HIV-1 protease activity, with IC₅₀ values of 18.7 μM.¹⁹ Nitric oxide and prostaglandin E₂, which caused inflammation, were inhibited with IC₅₀ values of 0.175 and 0.0195 μM, respectively.¹⁵

Supercritical carbon dioxide (CO₂) extraction is a novel option for the extraction process of herbal medicines owing to its benefit of being clean, safe, reusable, and compatible when compared to the old approach, such as solvent extraction and distillation.²⁰ Supercritical CO₂ extraction results in a higher concentration of nonpolar compounds in the final product, which is compliant with lipophilicity compounds like panduratin A.²¹ We collaborated with the Chao Phraya Abhaibhubejhr Hospital Foundation to develop supercritical CO₂ extraction of fingerroot, which increased the percentage of panduratin A to 15.0%. Our previous sub-chronic toxicity study showed that the administration of 25–100 mg/kg/day of fingerroot extract formulation in rats for 90 days showed no evidence of toxicity or mortality.²² Therefore, a dose of 45 mg/kg/day of panduratin A-consisted fingerroot extract was administered to examine absolute oral bioavailability, tissue distribution, metabolism, and excretion recovery in rats. In our previous study, healthy dogs were injected with 1 mg/kg/day of pure panduratin A and fed with 5 and 10 mg/kg/day of panduratin A-consisted

fingerroot extract formulation that showed acceptable pharmacokinetic parameters and possible metabolic pathways.²³ Other research groups have reported pharmacokinetic studies of panduratin A in fingerroot extract using ethanolic extraction with 5–10% w/w in animal models.²⁴ However, there is a lack of information comparing oral administration of pure panduratin A and panduratin A-consisted fingerroot extract. Due to a limited supply of pure panduratin A, we could not experiment with dogs. Therefore, small animals such as rats were selected for this study. We experimented using supercritical CO₂ extraction of fingerroot extract with a concentration of 15% w/w panduratin A. The tissue distribution study of panduratin A-consisted fingerroot extract was conducted in rats for 7 consecutive days. All major tissues related to COVID-19 infection, such as lungs, heart, and brain, were collected to determine panduratin A level. The extract of fingerroot that has been enriched can potentially lower the required dosage, minimize adverse effects of water-soluble minor components, enhancing patient compliance. With the potential for enriched fingerroot extract, this medicinal plant could be developed as a complementary or alternative medicine for COVID-19 treatment. Obtaining pharmacokinetic profile data is a crucial step towards advancing phytopharmaceutical development.

Materials and Methods

Chemicals and Materials

Supercritical CO₂ extraction of 15.0% w/w panduratin A-consisted fingerroot, as determined by liquid chromatography-tandem mass spectrometry (LCMS) analysis, and production of panduratin A (purity >93.6%) was performed by the Chao Phraya Abhaibhubejhr Hospital Foundation, Thailand (Figure 1). Dimethyl sulfoxide was purchased from Merck, Germany. Panduratin A standard reference with >98% purity was purchased from Biosynth Carbosynth, UK. A glycyrrhizin standard reference with >90% purity was purchased from Wako Pure Chemical Industries, Japan. Aerrane (Isoflurane USP), was purchased from Baxter Healthcare Corporation, USA.

Supercritical CO₂ Extraction of Fingerroot

Dried powder of fingerroot rhizome with moisture less than 3.5% w/w was extracted by supercritical carbon dioxide extraction. The extraction was conducted using a supercritical fluid extractor under optimal extraction conditions in the industrial process, which the Chao Phraya Abhaibhubejhr Hospital Foundation carried out. A yellow extract with an approximate extraction yield of 5% w/w was collected, and stored at 4°C until analysis.

Animals

Male Wistar rats aged 8–12 weeks and weighing approximately 400 g were obtained from the Chulalongkorn University Laboratory Animal Center (CULAC), Chulalongkorn University. The rats were housed in a controlled environment with a temperature of 20–24°C, relative humidity of 30–70%, and a 12:12 h light/dark cycle. Food and water were available *ad libitum*. The rats were fasted 12 h before the experiment and had free access to water. After administration of the test substances, the rats were placed in metabolic cages until 72 h post-administration. All animal experiments were approved

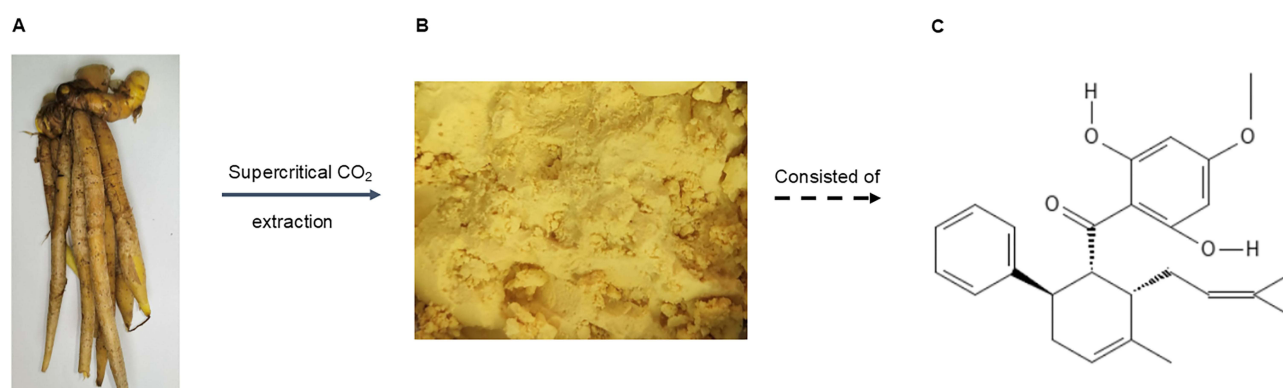


Figure 1 The physical appearance of (A) the fingerroot rhizome, (B) supercritical CO₂ fingerroot extract, and (C) panduratin A chemical structure.

by the Institutional Animal Care and Use Committee of the CULAC, Chulalongkorn University, Bangkok, Thailand (Protocol number 2173003, Approval date: March 12, 2021). The experiments were conducted under the guidelines for the Care and Use of Laboratory Animals and were conducted in compliance with the ARRIVE guidelines.^{25,26}

Pharmacokinetic Experiments

Rats were randomly divided into four groups (n=5 per group). For intravenous injections, single doses of 4.5 mg/kg pure panduratin A solution in 50% dimethyl sulfoxide were freshly prepared and then injected via the lateral tail vein of the rats. For oral administration, single doses of 45 mg/kg pure panduratin A or 45 mg/kg panduratin A-consisted fingerroot extract were fed to rats once, except for the group that received multiple doses of 45 mg/kg panduratin A-consisted fingerroot extract, which was fed once daily for 7 consecutive days to investigate panduratin A accumulation. The stock solutions of panduratin A for injection and oral administration were prepared using 50% DMSO to achieve the final concentration of 9 and 45 mg/mL, respectively. Before blood collection, rats were induced into the anesthetic state using a small animal anesthesia machine (Model R500IP; RWD Life Science, China). Rats were put in an induction chamber with 2–3% isoflurane vaporized by 1.0 L/min of oxygen and then transferred to a table while keeping light anesthesia by 1.0% isoflurane through a facial mask. A pre-heparinized syringe was used to collect 300 μ L of blood sample from the lateral tail vein on day 1 at 0 (pre-dose), 0.08, 0.25, 0.5, 1, 2, 4, 8, 24, 48, and 72 h and on day 7 at 0 (pre-dose), 0.08, 0.25, 0.5, 1, 2, 4, 8, 24, 48, as well as 72 h after test substance administration. The blood samples were centrifuged at 5000 g for 10 min at 4°C to collect plasma, which was then stored at –20°C until analysis. Urine and fecal samples were collected in metabolic cages 0–24 and 24–72 h after the administration of test substances. To verify the health status of the rats before and after administration, blood samples were collected at 0 and 24 h after administration of test substances and sent to the Small Animal Hospital, Faculty of Veterinary Science, Chulalongkorn University for blood tests to determine creatinine, alanine transaminase (ALT), and aspartate transaminase (AST) with normal range 0.2–0.7 mg/dL, 13–56 U/L, and 34–109 U/L, respectively.²⁷

Tissue Distribution Experiments

To investigate the tissue distribution of panduratin A, a total of 16 rats were randomly divided into four groups (n=4 per group) depending on the time point of sacrifice including 0 (pre-dose), 0.25, 1, and 4 h after dosing. The rats were orally administered 45 mg/kg panduratin A-consisted fingerroot extract daily for 7 consecutive days before sacrifice. The stock solution of panduratin A for oral administration was prepared by using 50% DMSO to achieve a final concentration of 45 mg/mL. Then, rats were euthanized with 30–40% isoflurane to collect nine tissues (brain, heart, kidney, liver, lung, spleen, stomach, small intestine, and large intestine). The tissue samples were washed with normal saline, dried with filter paper, weighed, and stored. Then, tissue samples were cut and weighed into 100 mg sections and mixed with 400 μ L of methanol in tubes containing 1.0-mm zirconia beads (BioSpec Products, USA) and homogenized using a BeadBug bead homogenizer (Benchmark Scientific, USA) at 4000 rpm for 2 min. The mixtures were then centrifuged at 5000 g for 5 min. The supernatant was transferred to a 1.7 mL tube and stored at –20°C until analysis.

Sample Preparation and Instrumentation

Feces were weighed into 100 mg sections and mixed with 400 μ L of methanol in tubes containing 1.0-mm zirconia beads (BioSpec Products, USA) and homogenized using a BeadBug bead homogenizer (Benchmark Scientific, USA) at 2000 rpm for 2 min. The mixtures were then centrifuged at 5000 g for 5 min. The supernatant was transferred to a 1.7 mL tube and stored at –20°C until analysis.

All biological samples (plasma, urine, feces, and organs) were processed by protein precipitation to extract panduratin A; 200 μ L of methanol with glycyrrhizin, used as an internal standard (IS), was added to 50 μ L of the biological sample, and the mixture was vortexed for 10 min. Then, the samples were centrifuged at 12,000 g for 10 min at 4°C, and 10 μ L of the supernatant was then injected into the LCMS instrument. Fecal samples were homogenized by adding methanol; then, the mixture was centrifuged at 1500 g for 10 min at 4°C to collect the supernatant. When the concentration of a biological sample exceeded the linear calibration curve, blank matrices were used to dilute the sample before protein precipitation.

The LCMS system consisted of an LCMS-8060 (Shimadzu, Japan) instrument equipped with a C18 reverse phase column (Synergi 4 μm Fusion-RP 80 \AA 50 \times 2 mm, Phenomenex, USA). The column temperature was maintained at 40°C, and analysis was performed using a mobile phase consisting of 0.2% formic acid in water (solvent A) and 100% methanol (solvent B) applied as a gradient (0–0.5 min, 10% B; 0.5–1.5 min, increase to 90% B; 1.5–2.5 min, 90% B; 2.5–3.5 min, decrease to 10% B; 3.5–4.5 min, 10% B) at a flow rate of 0.5 mL/min, with a 10 μL injection volume. A triple quadrupole mass spectrometer with negative mode electrospray ionization was used. The mass-to-charge ratios of panduratin A and glycyrrhizin were 405.10/165.90 and 821.25/350.90 Da, respectively. All operations were controlled and data acquisition and analysis were conducted using LabSolution software, version 5.86 (Shimadzu, Japan). The LCMS method was validated according to the guidance on bioanalytical method validation recommended by the USFDA.²⁸ The calibration curves of panduratin A were in the range of 0.98–1000 $\mu\text{g/L}$. The accuracy, precision, selectivity, specificity, linearity, recovery, matrix effect, and stability of the three quality control samples (10, 150, and 600 $\mu\text{g/L}$) were within a $\pm 15\%$ acceptable range. In addition, the lower limit of quantification (0.98 $\mu\text{g/L}$) was within a $\pm 20\%$ acceptable range (Figure S1-5 and Table S1-2).

An Agilent 6540 QTOF (Agilent Technologies, USA) coupled with an Agilent HPLC 1260 (Agilent Technologies, USA) was utilized for detecting the main metabolites of panduratin A in biological samples including plasma, urine, and feces of rats after intravenous administration with panduratin A 4.5 mg/kg. ZORBAX Eclipse Plus C18, 4.6 mm \times 100 mm, 3.5 μm column (Agilent Technologies, USA), was selected as the stationary phase at 35 °C. 0.1% formic acid in water (solvent A) and 0.1% formic acid in acetonitrile (solvent B) were applied as the mobile phase, with a following gradient system (0 min, 30% B; 0–20 min, increase to 90% B; 20–25 min, increase to 95% B; 25–30 min, 95% B), post-run 5 min, at a flow rate of 0.5 mL/min, with a 10 μL injection volume. The LCMS with positive and negative mode ionization with ESI were performed by inspecting a mass range of 100 to 1000 m/z at a scan rate of 4 spectra per second. The qualitative analysis of mass spectra was carried out using the Mass Hunter program version B.06.00 (Agilent Technologies, USA).

Data Analysis

PK solution software version 2.0 (Summit Research Services, USA) was used to perform a non-compartmental analysis of the pharmacokinetic parameters. The pharmacokinetic parameters in this study were as follows: maximum plasma concentration (C_{max}), time to reach the maximum plasma concentration (T_{max}), area under the plasma concentration–time curve from 0 to 72 h (AUC_{0-72}), area under the plasma concentration–time curve from time 0–infinity, absolute bioavailability, accumulation ratio, mean residence time (MRT), volume of distribution (Vd), total clearance (CL), and elimination half-life. Statistical analyses were performed using SPSS version 22.0 (IBM, USA). The normality of the data was determined using the Shapiro–Wilk test. A paired Student's *t*-test was used to determine significant differences in the health status of the rats. A Student's *t*-test or Mann–Whitney *U*-Test was used to determine significant differences in pharmacokinetic parameters between oral administration of pure panduratin A and fingerroot extract, and between oral administrations of fingerroot extract for 1 day and 7 days. The percentage recovery of panduratin A was estimated by dividing the total quantity of the test compound detected in urine or feces by the administered dosage. All data are expressed as the mean \pm standard deviation, except for the T_{max} and half-life, which are expressed as the median (IQR). Differences were considered significant at $p < 0.05$.

Results

Tolerability of Drug Administration by Rats

The health status of the rats during the experiment was evaluated by observing their physical appearance, monitoring their weight, and collecting blood both before and after intravenous administration of panduratin A or oral administration of panduratin A and fingerroot extract. None of the rats showed a significant change in physical appearance or weight. The kidney and liver function values also showed no significant differences between the pre-dose and post-dose values in any group (Table 1). Consecutive oral dosing of fingerroot extract for 7 days did not result in toxicity or abnormalities in rats.

Table 1 Physical and Biochemical Profiles of Experimental Rats

Biochemical parameters	Normal range	Experimental groups				
		Baseline	Panduratin A 4.5 mg/kg i.v.	Panduratin A 45 mg/kg p.o. Day 1	Fingerroot extract (panduratin A 45 mg/kg) p.o. Day 1	Fingerroot extract (panduratin A 45 mg/kg) p.o. Day 7
Physical appearance		Normal	Normal	Normal	Normal	Normal
Weight (g)		413 ± 12	415 ± 15	418 ± 11	410 ± 20	414 ± 8
Creatinine (mg/dL)	0.2–0.7	0.3 ± 0.1	0.2 ± 0.1	0.3 ± 0.1	0.3 ± 0.1	0.2 ± 0.1
ALT (U/L)	13–56	34 ± 6	39 ± 4	29 ± 3	32 ± 4	33 ± 3
AST (U/L)	34–109	73 ± 7	71 ± 9	77 ± 5	75 ± 7	80 ± 9

Notes: Data are expressed as mean ± SD, (n = 5); Decimal numbers were reported according to laboratory standards of Small Animal Hospital, Faculty of Veterinary Science, Chulalongkorn University.

Abbreviations: AST, aspartate transaminase; ALT, alanine transaminase.

Plasma Concentration-Time Profiles

The plasma concentration–time profiles of panduratin A after intravenous administration of panduratin A and oral administration of panduratin A and fingerroot extract are shown in Figure 2. After intravenous administration of 4.5 mg/kg pure panduratin A, the plasma concentration reached a maximum of approximately 20,000 µg/L obtained using the extrapolation from PK solution software, and then decreased to 500 µg/L after 72 h. After a single oral administration of 45 mg/kg pure panduratin A, the plasma concentration reached a maximum of approximately 5000 µg/L and then decreased to 500 µg/L after 72 h. After a single oral administration of 45 mg/kg panduratin A-consisted fingerroot extract, the plasma concentration reached a maximum of approximately 3000 µg/L and then decreased to 200–300 µg/L after 72 h. After 7 consecutive days of oral administration of the fingerroot extract, the T_{max} of panduratin A was not significantly different from the first day of administration. The accumulation ratio of panduratin A was approximately 1.47 after oral administration of fingerroot extract for 7 consecutive days.

Pharmacokinetic Parameters

The pharmacokinetic parameters of panduratin A for all experimental groups are listed in Table 2. A single oral dose of 45 mg/kg panduratin A-consisted fingerroot extract showed a significantly lower AUC than a single oral dose of 45 mg/

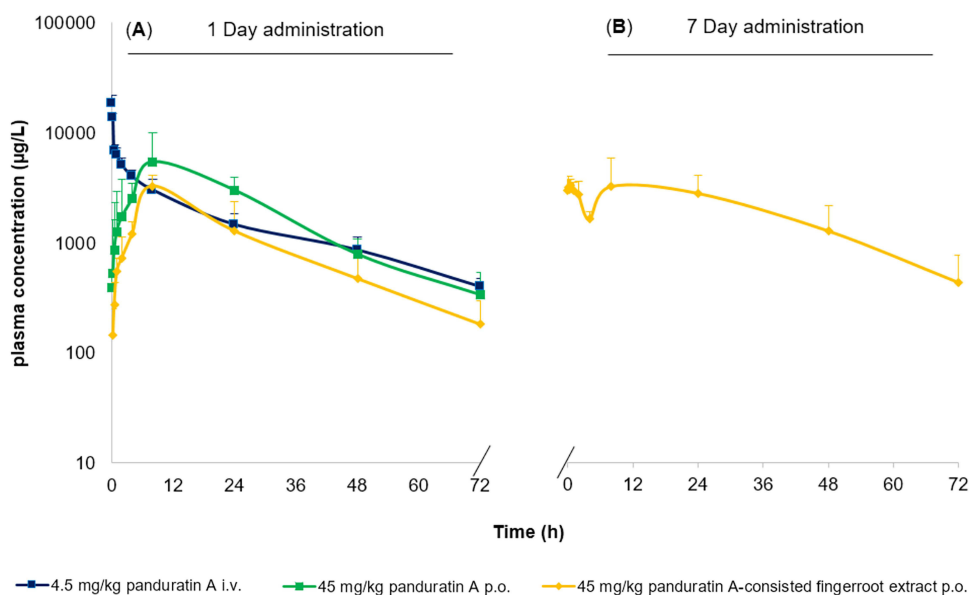


Figure 2 Plasma concentration-time profile of panduratin A after intravenous dosing as 4.5 mg/kg pure panduratin A, and oral dosing as 45 mg/kg pure panduratin A, and 45 mg/kg panduratin A-consisted fingerroot extract. (A) single administration on day 1. (B) multiple administration for 7 consecutive days.

Table 2 Pharmacokinetic Parameters of Panduratin a After Intravenous Injection of 4.5 Mg/Kg Panduratin a, Oral Administration of 45 Mg/Kg Panduratin a, and 45 Mg/Kg Panduratin a-Consisted Fingerroot Extract as Single and Repeated Doses

Pharmacokinetic parameters	Panduratin A			
	Panduratin A 4.5 mg/kg i.v.	Panduratin A 45 mg/kg p.o. Day 1	Fingerroot extract (panduratin A 45 mg/kg) p.o. Day 1	Fingerroot extract (panduratin A 45 mg/kg) p.o. Day 7
C_{max}^a ($\mu\text{g/L}$)	18,367 \pm 3594	4833 \pm 659	3269 \pm 819*	3608 \pm 713**
T_{max}^b (h)	N/A	8.00 (0.25)	8.00 (0.25)	8.00 (0.25)
AUC_{0-72}^a ($\mu\text{g}\cdot\text{h/L}$)	130,706 \pm 19,457	132,309 \pm 33,525	77,086 \pm 32,119*	113,194 \pm 20,100**
$AUC_{0-\infty}^a$ ($\mu\text{g}\cdot\text{h/L}$)	152,296 \pm 30,227	138,223 \pm 37,673	87,581 \pm 31,691*	132,614 \pm 33,945**
Absolute bioavailability ^c (%)	N/A	9.08	5.75	N/A
Accumulation ratio ^d	N/A	N/A	N/A	1.47
MRT ^a (h)	32.53 \pm 8.81	43.55 \pm 13.50	45.07 \pm 10.45	53.83 \pm 17.06
Vd ^a (L/kg)	1.28 \pm 0.39	7.16 \pm 1.75	13.21 \pm 4.35*	11.38 \pm 2.70**
CL ^a (L/h/kg)	0.03 \pm 0.01	0.29 \pm 0.10	0.57 \pm 0.20*	0.36 \pm 0.10**
Half-life ^b (h)	23.51 (3.19)	17.70 (1.90)	17.40 (3.65)	21.50 (2.61)

Notes: ^a Data are expressed as mean \pm SD; ^b Data are expressed as median (IQR); ^c Absolute bioavailability was calculated as $(AUC_{P.O.}/DOSE_{P.O.})/(AUC_{i.v.}/DOSE_{i.v.}) \times 100$; ^d Accumulation ratio was calculated as AUC_{0-72} at day 7/ AUC_{0-72} at day 1; * $P < 0.05$ for significant differences from panduratin A 45 mg/kg P.O.; ** $P < 0.05$ for significant differences from CO₂ fingerroot extract P.O. Day 1; C_{max} : maximum plasma concentration; T_{max} : time to reach C_{max} ; AUC_{0-72} : area under the plasma concentration–time curve from time 0–72 h; $AUC_{0-\infty}$: area under the plasma concentration–time curve from time 0-infinity; MRT: mean resident time; Vd: volume of distribution; CL: clearance.

kg pure panduratin A, with absolute oral bioavailability of approximately 6 and 9%, respectively. While MRT and half-life exhibited no difference between fingerroot extract and pure panduratin A group. However, the Vd and CL of the fingerroot extract group were higher than the pure panduratin A group ($p < 0.05$). The pharmacokinetic parameters after multiple oral administrations of fingerroot extract exhibited significantly higher AUC compared with those obtained after a single administration, with an accumulation ratio of 1.47. While MRT and half-life showed no difference, Vd and CL were lower than a single administration ($p < 0.05$).

Tissue Distribution Profiles

The tissue distribution profiles of panduratin A-consisted fingerroot extract in rats at different time points are shown in Figure 3. Panduratin A could be detected in all collected organs, including the brain. The highest tissue-to-plasma ratio of panduratin A was 100-fold in the stomach within 15 min (0.25 h). The concentrations in organs other than gastrointestinal organs were approximately 1–10 fold within 15 min (0.25 h). In the kidney, the concentration was approximately 0.1-fold within 15 min (0.25 h). In other major organs including the lung, heart, and spleen, the concentration was approximately 1–10 fold within 15 min (0.25 h). No differences were observed in the tissue-to-plasma ratios among samples from the same organs collected at 0.25, 1, and 4 h. The Results indicated that panduratin A was widely distributed in the gastrointestinal tract and major organs, especially lungs and heart which were targeted organs for anti-SARS-CoV-2 and anti-inflammatory.

Biotransformation and Excretion

Using QTOF LCMS analysis, three panduratin A metabolites were observed in feces, 0–24 h after intravenous injection of pure panduratin A 4.5 mg/kg (Figure 4). Two major peaks in the feces samples at 0–24 h were detected as hydrogen deduct with oxidation $[M-H]^- + OH$ of panduratin A, by observing that the molecules had the same molecular weight (421.18 g/mol) but distinct retention times (14.97 and 15.62 min), we concluded that the molecules were the same deduct with a different attachment of the hydroxyl group. Another major peak in the feces samples at 0–24 h was deduced to be a hydrogen deduct with dioxidation $[M-H]^- + 2OH$ of panduratin A, with a molecular weight of 437.1835 g/mol and a retention time of 10.89 min. However, none of the metabolites of panduratin A were detected in plasma or urine as determined by QTOF LCMS under the experiment conditions.

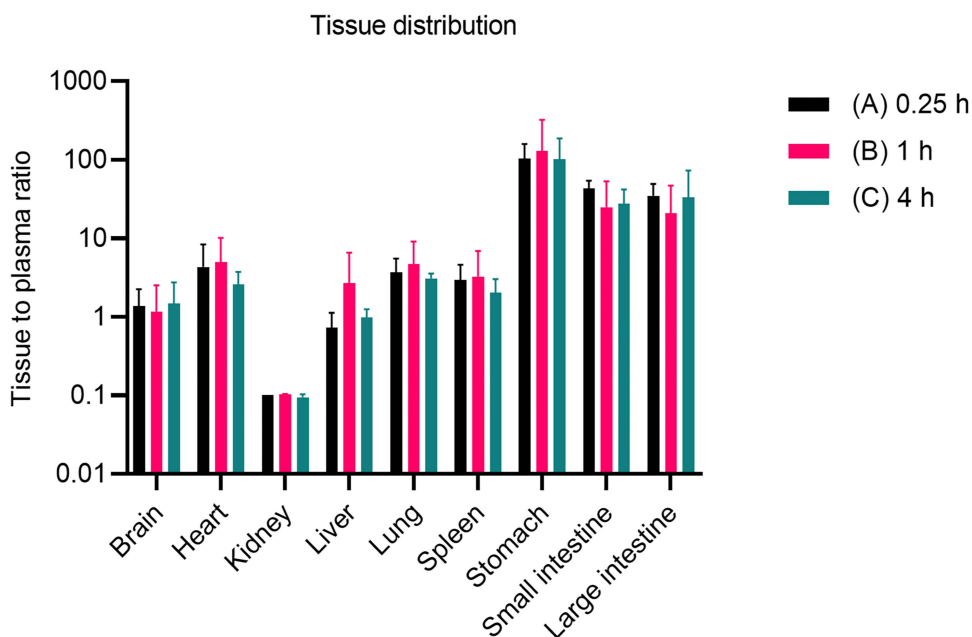


Figure 3 Tissue to plasma ratio of panduratin A in internal organs at (A) 0.25, (B) 1, and (C) 4 h after oral dosing as 45 mg/kg panduratin A-consisted fingerroot extract.

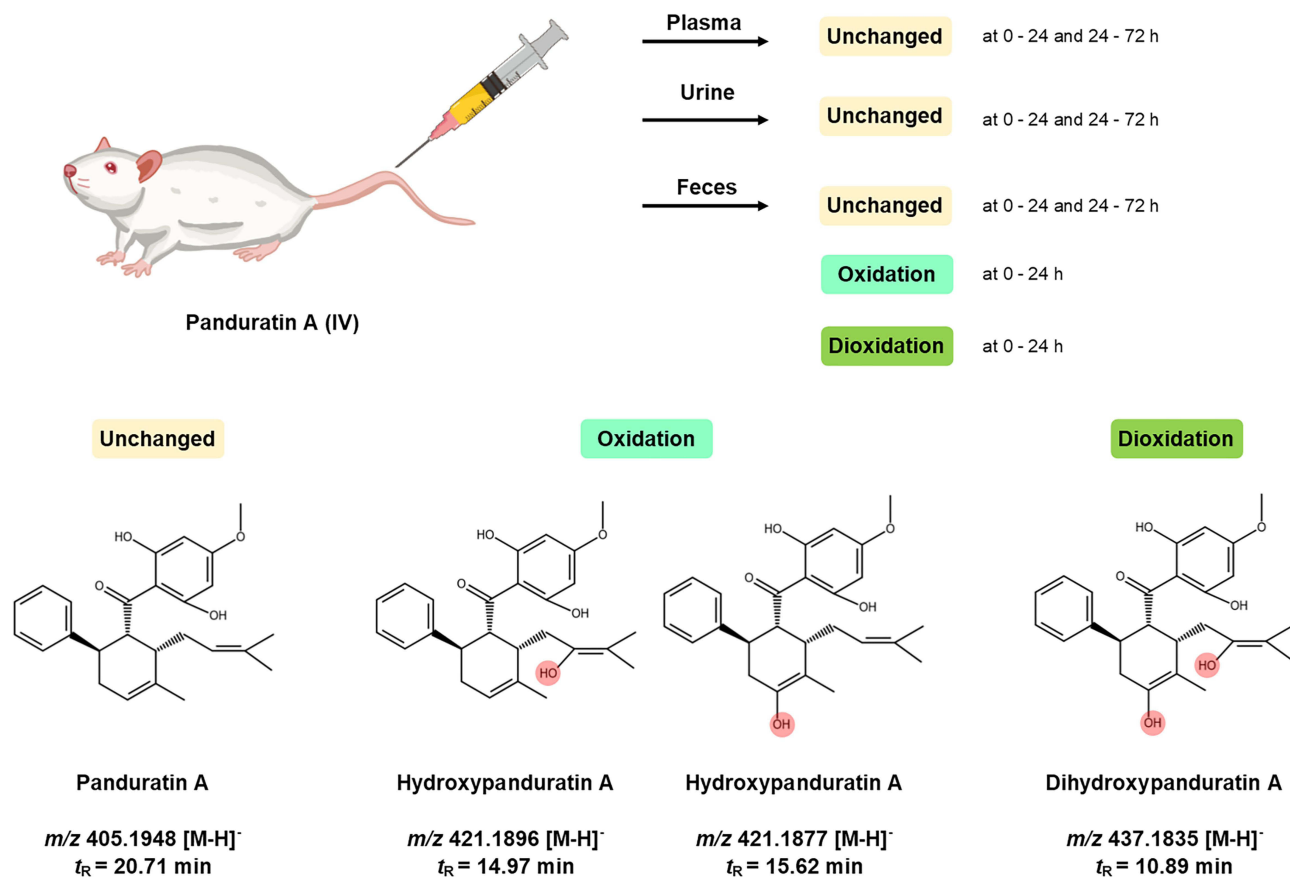


Figure 4 Biotransformation and excretion route of panduratin A in rats.

Table 3 The Percentage Recovery of Panduratin a in Excreta of All Experimental Groups

Percent recovery (% from administered dose)	Experimental groups							
	Panduratin A 4.5 mg/kg i.v.		Panduratin A 45 mg/kg p.o. Day 1		Fingerroot extract (panduratin A 45 mg/kg) p.o. Day 1		Fingerroot extract (panduratin A 45 mg/kg) p.o. Day 7	
	0–24 h	24–72 h	0–24 h	24–72 h	0–24 h	24–72 h	0–24 h	24–72 h
Urine Panduratin A	0.70 ± 0.25	1.42 ± 0.54	0.07 ± 0.02	0.15 ± 0.04	11.02 ± 0.88	2.23 ± 0.34	10.41 ± 1.09	0.81 ± 0.29
Feces Panduratin A	17.47 ± 1.56	7.66 ± 0.38	13.31 ± 0.95	8.21 ± 0.49	26.96 ± 4.02	5.63 ± 0.77	43.16 ± 5.97	16.70 ± 1.12

Notes: Data are expressed as mean ± SD, (n = 5).

After intravenous administration of pure panduratin A, a portion of panduratin A was excreted unchanged via the feces within 0–72 h (25% of the administered dose). However, only negligible amounts of unchanged panduratin A were excreted in the urine within 0–72 h (2% of the administered dose). Similarly, for oral administration of pure panduratin A, approximately 22% and 1% of the administered dose was excreted unchanged in the feces and urine, respectively, within 0–72 h. However, an increased amount of unchanged panduratin A excretion in both feces and urine within 0–72 h (33% and 13% of the administered dose, respectively) was observed with oral administration of the fingerroot extract. In the group that received oral administration of the fingerroot extract for 7 days, the amount of unchanged panduratin A excreted via the feces was most significantly increased (60% of the administered dose), and no difference in the amount excreted in the urine was observed (11% of the administered dose), as shown in Table 3.

Discussion

In a previous *in vitro* study, fingerroot extract and panduratin A inhibited SARS-CoV-2 infection.⁷ Furthermore, an *in vivo* study showed that fingerroot extract could reduce the severity of lung pathology in infected hamsters.⁸ To continue clinical trials, preclinical data including the efficacy, toxicity, and pharmacokinetics of panduratin A are necessary.²⁹ In this study, the pharmacokinetic parameters of panduratin A as a pure compound and in a fingerroot extract were determined using a rat model. All experimental animals tolerated the test compounds after either intravenous or oral administration and showed no abnormalities or signs of toxicity. This finding indicated the safety of the administration of the treatment compounds within the examined dosing range. The results are consistent with those of another toxicity study in which 60–240 mg/kg of fingerroot extract was orally administered to rats for 60 days, resulting in no notable changes in weight, blood, biochemical profiles of liver and kidney function, or histology.³⁰ Moreover, functional dyspepsia patients who received 350 mg of fingerroot extract three times per day for 1 month tolerated treatment and showed no change in gastric histopathology.³¹ These results indicate the safety of fingerroot extract in animals and humans to some extent.

The C_{max} of panduratin A after oral administration of 45 mg/kg pure panduratin A surpassed the IC_{50} value, by approximately 15-fold, of that obtained in an *in vitro* study using SARS-CoV-2, while the minimum plasma concentration at 24 h remained approximately 10-fold higher than the IC_{50} value.⁷ Meanwhile, the C_{max} of panduratin A after oral administration of 45 mg/kg of panduratin A-consisted fingerroot extract surpassed the IC_{50} value by approximately 10-fold of that obtained in an *in vitro* study using SARS-CoV-2, and the minimum plasma concentration at 24 h remained approximately 4-fold higher than the IC_{50} value. The absolute oral bioavailability values of pure panduratin A and that in fingerroot extract were approximately 9% and 6%, respectively. Differences in pharmacokinetic profiles were observed between pure panduratin A and that in fingerroot extract. The fingerroot extract exhibited a lower C_{max} , lower AUC, higher Vd, and faster CL than those of pure panduratin A. These differences might be caused by the supercritical CO₂ extraction process, in that the non-polar property of CO₂ increases the solubilization of lipophilic substances such as panduratin A.²¹ However, high lipophilicity causes low water solubility and low oral absorption.³² Additionally, the high lipophilicity and low solubility of CO₂ fingerroot extract resulted in decreased absorption and increases in distribution, metabolism, and excretion.³³ These differences in pharmacokinetic profiles could result from differences in extraction

methods from fingerroot. Extraction techniques were reported to influence the quantity of active substances and the diversity of minor compounds, which resulted in differences in the pharmacokinetic parameters.³⁴ The difference of C_{max} and T_{1/2} in our previous study in dogs, might be caused by various factors e.g. we used fingerroot extract formulation with improved water solubility in a solid dosage form for the dog study, but in the rat study we used fingerroot extract in liquid dosage form. Therefore, the maximum concentration of different preparations could result in the difference of C_{max}. In addition, interspecies differences especially in clearance and elimination half-life are common phenomena among mammal species such as small rodents (rats) and large animals (dogs). In another study on a different species treated with a fingerroot extract, the difference in elimination half-life has also been reported.²⁴ According to Lipinski's rule of five,³⁵ panduratin A does not completely comply with the rule because of its high logP value, which may cause low water solubility and affect its oral bioavailability. Natural compounds from medicinal plants usually have low water solubility and high lipophilicity, which results in inadequate absorption and bioavailability. The addition of inactive substances and different formulations could enhance water solubility and improve bioavailability.³⁶ For the biopharmaceutical classification system (BCS), panduratin A is considered a BCS class II drug, with low solubility but high permeability.³⁷ To overcome the limitation, surfactants, complexing agents, or nanoparticle formulation might be required.³⁷ Potentially, to develop solid dosage medication for humans, cyclodextrin is used as an inactive ingredient to improve the water solubility and bioavailability of drugs or herbal medicines and is safe in animals and humans.³⁸ Cyclodextrin improved the water solubility and bioavailability of methoxyflavones from *Kaempferia parviflora* Wall. ex Baker extract.³⁹ In addition, the Inclusion complex of zerumbone isolated from *Zingiber zerumbet* (L). Roscoe ex Sm with hydroxypropyl- β -cyclodextrin improved the solubility with water.⁴⁰ By promoting water solubility, the bioactive substances could be more readily absorbed, resulting in increases in plasma levels and oral bioavailability.⁴¹

Oral administration of fingerroot extract from CO₂ extraction has the potential to maximize clinical benefits, including decreased duration of COVID-19 and reduced post-acute sequelae of SARS-CoV-2 infection, as well as limited adverse effects from water-soluble minor components. However, the low oral bioavailability of panduratin A poses a challenge to its anti-SARS-CoV-2 efficacy.⁴² Panduratin A is highly lipophilic¹⁸ and tends to be distributed in the tissue rather than circulating in the blood vessels. In the present study, panduratin A accumulation mainly occurred in the gastrointestinal organs, which could have been caused by its high lipophilicity and route of administration. Normally, lipophilic compounds exhibit a large tissue distribution.³³ The lowest tissue-to-plasma ratio was found in the kidney, which is consistent with the high lipophilicity of panduratin A. In another study, oral administration of ethanolic fingerroot extract to rats revealed the distribution of panduratin A in various tissues, mainly including the skin, lungs, and heart.⁴³ In our study, panduratin A was found in all major organs including the lung, heart, spleen, and brain which were targets for COVID-19 manifestations. The difference between the kidney distribution of panduratin A in another study,⁴³ might be caused by various factors e.g. extraction method (solvent or supercritical CO₂ extraction) which causes a difference in minor compounds, rat species (Sprague-Dawley or Wistar), dosage, or solvent vehicle (corn oil or DMSO). In addition, differences in vehicle use also affected the pharmacokinetic parameters, especially the absorption and bioavailability.⁴⁴ The lung is mainly related to SARS-CoV-2 infection with angiotensin-converting enzyme 2 receptors as a key binding target.⁴⁵ In COVID-19 patients, cardiovascular diseases have been correlated with severe complications, while neurological symptoms have been reported during and after the infection.^{46,47} Panduratin A exhibits anti-inflammatory effects, COVID-19 causes inflammation due to infection and cytokine storm in the host.^{8,48} Thus, the existence of panduratin A in these organs shows a potential for a COVID-19 treatment. With the concept of combination drug therapies, this natural remedy could serve as a starting point for further drug development in treating these lung diseases.⁴⁹

Panduratin A was predominantly biotransformed after the intravenous injection of the test compound and was excreted as biotransformed products within 24 hours. The QTOF LCMS analysis revealed that panduratin A metabolites were present in the feces, which decreased its lipophilicity by adding a hydroxyl group resulting in decreased retention time of reversed-phase chromatography. However, the glucuronidation form of panduratin A was not detected in rats but could be found in dogs.²³ The differences in glucuronidation activity between species could be observed even between rodent species.⁵⁰ It is noteworthy that the potential biotransformation of Panduratin A has been observed to consist of Phase I metabolism, specifically oxidation. This metabolic process enhanced the solubility of the compound in water and assisted excretion of the xenobiotics such as panduratin A from the mammal body. The

panduratin A excretion results were consistent with the tissue distribution profiles and the high lipophilicity of panduratin A. The amount of panduratin A elimination via the urine was negligible, at approximately 1–10% of the administered dose, and excretion through the feces was dominant, at approximately 22–60% of the administered dose. Biliary excretion is expected to be the main route of elimination because bile acids allow solubilization of lipid-soluble substances.⁵¹ Thus, further pharmaceutical development is essential to improve the water solubility and bioavailability of panduratin A for the use of fingerroot extract as a phytopharmaceutical product.

Conclusion

Intravenous administration of panduratin A as a pure compound and oral administration of CO₂ fingerroot extract did not show toxicity in rats. The oral bioavailability of the fingerroot extract was slightly lower than that of pure panduratin A because of its high lipophilicity. Panduratin A was mostly distributed in the gastrointestinal organs and was mainly excreted via the fecal route. The main metabolites of panduratin A detected in feces were oxidation and dioxidation products. Furthermore, the impact of food on the absorption of panduratin A as a lipophilic compound should be investigated in future research. These pharmacokinetic results could promote further phytopharmaceutical development of fingerroot extract for clinical applications.

Abbreviations

ALT, Alanine aminotransferase; AST, Aspartate aminotransferase; AUC, Area under the plasma concentration-time curve; BCS, Biopharmaceutical classification system; CL, Total clearance; C_{max}, Maximum plasma concentration; CO₂, Carbon dioxide; COVID-19, Coronavirus disease 2019; DMSO, Dimethyl sulfoxide; LCMS, Liquid chromatography tandem mass spectrometry; MRT, Mean residence time; QTOF, Quadrupole Time-of-Flight; SARS-CoV-2, Severe acute respiratory syndrome coronavirus 2; T_{max}, Time to reach maximum plasma concentration; USFDA, United States Food and Drug Administration; V_d, Volume of distribution.

Data Sharing Statement

The data that support the findings of this study are available from the corresponding author upon reasonable request. Some data may not be made available because of privacy or ethical restrictions.

Ethics Approval

The animal study protocol was approved by the Institutional Animal Care and Use Committee of the CULAC, Chulalongkorn University, Bangkok, Thailand (Protocol number 2173003; Approval date: March 12, 2021)

Acknowledgments

We thank the Chao Phraya Abhaibhubejhr Hospital Foundation for providing the fingerroot extract and panduratin A. We thank Lisa Kreiner, PhD, from Edanz (www.edanz.com/ac) for editing a draft of this manuscript.

Author Contributions

All authors made a significant contribution to the work reported, whether that is in the conception, study design, execution, acquisition of data, analysis, and interpretation, or all these areas; took part in drafting, revising, or critically reviewing the article; gave final approval of the version to be published; have agreed on the journal to which the article has been submitted; and agree to be accountable for all aspects of the work.

Funding

This work was supported by the National Research Council of Thailand (to Suradej Hongeng) and the 60th Year Supreme Reign of His Majesty King Bhumibol Adulyadej Scholarship, Mahidol University (to Teetat Kongratanasert).

Disclosure

The authors declare no conflicts of interest.

References

1. Wang Z, Yang L. Chinese herbal medicine: fighting SARS-CoV-2 infection on all fronts. *J Ethnopharm.* 2021;270:113869.
2. Wang Z, Yang L, Zhao XE. Co-crystallization and structure determination: An effective direction for anti-SARS-CoV-2 drug discovery. *Comput Struct Biotechnol J.* 2021;19:4684–4701.
3. Wang Z, Yang L. The therapeutic potential of natural dietary flavonoids against SARS-CoV-2 Infection. *Nutrients.* 2023;15(15):3443.
4. Yang L, Wang Z. Bench-to-bedside: innovation of small molecule anti-SARS-CoV-2 drugs in China. *Eur J Med Chem.* 2023;257:115503.
5. Onyeaghala AA, Anyiam AF, Husaini DC, Onyeaghala EO, Obi E. Herbal supplements as treatment options for COVID-19: a call for clinical development of herbal supplements for emerging and re-emerging viral threats in Sub-Saharan Africa. *Sci Afr.* 2023;20:e01627.
6. Al-Kuraisy HM, Al-Fakhrany OM, Elekhawy E, et al. Traditional herbs against COVID-19: back to old weapons to combat the new pandemic. *Eur J Med Res.* 2022;27(1):186.
7. Kanjanasirirat P, Suksatu A, Manopwisedjaroen S, et al. High-content screening of Thai medicinal plants reveals *Boesenbergia rotunda* extract and its component Panduratin A as anti-SARS-CoV-2 agents. *Sci Rep.* 2020;10(1):19963.
8. Kongratanasert T, Kongsomros S, Arya N, et al. Pharmacological activities of fingerroot extract and its phytoconstituents against SARS-CoV-2 infection in golden Syrian hamsters. *J Exp Pharmacol.* 2023;15:13–26.
9. Eng-Chong T, Yean-Kee L, Chin-Fei C, et al. *Boesenbergia rotunda*: From ethnomedicine to drug discovery. *eCAM.* 2012;2012:473637.
10. Yun J-M, Kweon M-H, Kwon H, Hwang J-K, Mukhtar H. Induction of apoptosis and cell cycle arrest by a chalcone panduratin A isolated from *Kaempferia pandurata* in androgen-independent human prostate cancer cells PC3 and DU145. *Carcinogenesis.* 2006;27(7):1454–1464.
11. Kiat TS, Phippen R, Yusof R, Ibrahim H, Khalid N, Rahman NA. Inhibitory activity of cyclohexenyl chalcone derivatives and flavonoids of fingerroot, *Boesenbergia rotunda* (L.), towards dengue-2 virus NS3 protease. *Bioorg Med Chem Lett.* 2006;16(12):3337–3340.
12. Rukayadi Y, Han S, Yong D, Hwang J-K. *In vitro* antibacterial activity of panduratin A against *Enterococci* clinical isolates. *Biol Pharm Bull.* 2010;33(9):1489–1493.
13. Sohn JH, Han K-L, Lee S-H, Hwang J-K. Protective effects of panduratin A against oxidative damage of *tert*-butylhydroperoxide in human HepG2 cells. *Biol Pharm Bull.* 2005;28(6):1083–1086.
14. Thongnuanjan P, Soodvilai S, Fongsupa S, et al. Protective effect of panduratin A on cisplatin-induced apoptosis of human renal proximal tubular cells and acute kidney injury in mice. *Biol Pharm Bull.* 2021;44(6):830–837.
15. Yun J-M, Kwon H, Hwang J-K. *In vitro* anti-inflammatory activity of panduratin A isolated from *Kaempferia pandurata* in RAW264.7 cells. *Planta Med.* 2003;69(12):1102–1108.
16. Pattaratanawadee E, Rachtanapun C, Wanchaitanawong P, Mahakarnchanakul W. Antimicrobial activity of spice extracts against pathogenic and spoilage microorganisms. *Kasetsart J Nat Sci.* 2006;40:159–165.
17. Mohan S, Hobani YH, Shaheen E, et al. Ameliorative effect of Boesenbergin A, a chalcone isolated from *Boesenbergia rotunda* (Fingerroot) on oxidative stress and inflammation in ethanol-induced gastric ulcer *in vivo*. *J Ethnopharm.* 2020;261:113104.
18. Panduratin A, PubChem. PubChem Compound Summary for CID 6483648, National Center for Biotechnology Information; Available from <https://pubchem.ncbi.nlm.nih.gov/compound/Panduratin-A#section=Chemical-and-Physical-Properties>. Accessed December 6, 2023.
19. Cheenpracha S, Karalai C, Ponglimanont C, Subhadhirasakul S, Tewtrakul S. Anti-HIV-1 protease activity of compounds from *Boesenbergia pandurata*. *Bioorg Med Chem.* 2006;14(6):1710–1714.
20. Abd Hamid IA, Ismail N, Abd Rahman N. Supercritical carbon dioxide extraction of selected herbal leaves: An overview. *IOP Conf Ser Mater Sci Eng.* 2018;358(1):012037.
21. Sahena F, Zaidul ISM, Jinap S, et al. Application of supercritical CO₂ in lipid extraction – a review. *J Food Eng.* 2009;95(2):240–253.
22. Techapichetvanich P, Tangpanithandee S, Supannapan K, Wongwivatthanakut S, Chang LC, Khemawoot P. Oral sub-chronic toxicity of fingerroot (*Boesenbergia rotunda*) rhizome extract formulation in Wistar rats. *Toxicol Rep.* 2024;12:224–233.
23. Boonyarattanasoonthorn T, Kongratanasert T, Jiso A, et al. Absolute oral bioavailability and possible metabolic pathway of panduratin A from *Boesenbergia rotunda* extract in beagle dogs. *Pharm Biol.* 2023;61(1):590–597.
24. Choi S, Kim C, Son H, Hwang JK, Kang W. Estimation of an appropriate human dose of *Boesenbergia pandurata* extracts based on allometric scaling data of panduratin A in mice, rats, and dogs. *J Med Food.* 2020;23(4):453–458.
25. National Research Council (US). Committee for the update of the guide for the care and use of laboratory animals. 8. In: *Guide for the Care and Use of Laboratory Animals*. Washington (DC): National Academies Press (US); 2011.
26. du Sert N P, Hurst V, Ahluwalia A, et al. The ARRIVE guidelines 2.0: Updated guidelines for reporting animal research. *PLoS Biol.* 2020;18(7).
27. Kurtz DM, Travlos GS. *The Clinical Chemistry of Laboratory Animals*. 3rd ed. CRC Press; 2017.
28. U.S. Food and Drug Administration [USFDA]. Bioanalytical method validation - guidance for industry. U.S. Food and Drug Administration; 2018; Available from <https://www.fda.gov/files/drugs/published/Bioanalytical-Method-Validation-Guidance-for-Industry.pdf>. Accessed December 6, 2023.
29. Reichel A, Lienau P. Pharmacokinetics in drug discovery: an exposure-centred approach to optimising and predicting drug efficacy and safety. *Handb Exp Pharmacol.* 2016;232:235–260.
30. Saraithong P, Saenphet S, Saenphet K. Safety evaluation of ethanol extracts from *Boesenbergia rotunda* (L.) Mansf. in male rats. *Tren Res Sci Tech.* 2010;2(1):19–22.
31. Chitapanarux T, Lertprasertsuke N, Toworakul C. Efficacy and safety of fingerroot (*Boesenbergia rotunda*) extract in patients with functional dyspepsia: a randomized, placebo-controlled trial. *Digestion.* 2021;102(4):599–606.
32. Wils P, Warnery A, Phung-Ba V, Legrain S, Scherman D. High lipophilicity decreases drug transport across intestinal epithelial cells. *J Pharmacol Exp Ther.* 1994;269(2):654–658.
33. Alavijeh MS, Chishty M, Qaiser MZ, Palmer AM. Drug metabolism and pharmacokinetics, the blood-brain barrier, and central nervous system drug discovery. *NeuroRx.* 2005;2(4):554–571.
34. Sun S, Wang Y, Wu A, Ding Z, Liu X. Influence factors of the pharmacokinetics of herbal resourced compounds in clinical practice. *eCAM.* 2019;2019:1983780.
35. Lipinski CA, Lombardo F, Dominy BW, Feeney PJ. Experimental and computational approaches to estimate solubility and permeability in drug discovery and development settings. *Adv Drug Deliv Rev.* 1997;23(1):3–25.
36. Kesarwani K, Gupta R, Mukerjee A. Bioavailability enhancers of herbal origin: an overview. *Asian Pac J Trop Biomed.* 2013;3(4):253–266.

37. Samineni R, Chimakurthy J, Konidala S. Emerging Role of Biopharmaceutical Classification and Biopharmaceutical Drug Disposition System in Dosage form Development: a Systematic Review. *Turk J Pharm Sci.* 2022;19(6):706–713.
38. European Medicines Agency [EMA]. Cyclodextrins used as excipients. European Medicines Agency. Available from https://www.ema.europa.eu/en/documents/scientific-guideline/questions-answers-cyclodextrins-used-excipients-medicinal-products-human-use_en.pdf. Accessed December 6, 2023.
39. Mekjaruskul C, Yang YT, Leed MG, Sadgrove MP, Jay M, Sripanidkulchai B. Novel formulation strategies for enhancing oral delivery of methoxyflavones in *Kaempferia parviflora* by SMEDDS or complexation with 2-hydroxypropyl- β -cyclodextrin. *Int J Pharm.* 2013;445(1–2).
40. Muhammad Nadzri N, Abdul AB, Sukari MA, et al. Inclusion complex of zerumbone with hydroxypropyl- β -cyclodextrin induces apoptosis in liver hepatocellular HepG2 cells via caspase 8/Bid cleavage switch and modulating Bcl2/Bax ratio. *Evid Bas Compl Alternat Med.* 2013;2013:810632.
41. Huang J, Liu Y, Li X, et al. Comparative pharmacokinetic profiles of five poorly soluble pulchinosides in different formulations from *Pulsatilla chinensis* saponins extracts for enhanced bioavailability. *Biomed Chromatogr.* 2015;29(12):1885–1892.
42. Wang Z, Yang L, X-q S. Oral GS-441524 derivatives: next-generation inhibitors of SARS-CoV-2 RNA-dependent RNA polymerase. *Front Immunol.* 2022;13:1015355.
43. Won J, Noh K, Hwang J-K, Shin BS, Kang W. Pharmacokinetics of panduratin a following oral administration of a *Boesenbergia pandurata* extract to rats. *J Food Drug Anal.* 2021;29(4):676–683.
44. Kim HJ, Bruckner JV, Dallas CE, Gallo JM. Effect of dosing vehicles on the pharmacokinetics of orally administered carbon tetrachloride in rats. *Toxicol Appl Pharmacol.* 1990;102(1):50–60.
45. Lopes-Pacheco M, Silva PL, Cruz FF, et al. Pathogenesis of multiple organ injury in COVID-19 and potential therapeutic strategies. *Front Physiol.* 2021;12.
46. Gavriatopoulou M, Korompoki E, Fotiou D, et al. Organ-specific manifestations of COVID-19 infection. *Clin Exp Med.* 2020;20(4):493–506.
47. Xu E, Xie Y, Al-Aly Z. Long-term neurologic outcomes of COVID-19. *Nat Med.* 2022;28(11):2406–2415.
48. Montazersaheb S, Hosseiniyan Khatibi SM, Hejazi MS, et al. COVID-19 infection: an overview on cytokine storm and related interventions. *Virolog J.* 2022;19(1):92.
49. Yang L, Wang Z. Natural products, alone or in combination with FDA-Approved Drugs, to Treat COVID-19 and lung cancer. *Biomedicines.* 2021;9(6):689.
50. Shiratani H, Katoh M, Nakajima M, Yokoi T. Species Differences in UDP-Glucuronosyltransferase Activities in Mice and Rats. *Drug Metab Dispos.* 2008;36(9):1745–1752.
51. Seng K-Y, Lee L. Drug distribution and drug elimination. In: Tarek AA, editor. *Basic Pharmacokinetic Concepts and Some Clinical Applications*. Rijeka: IntechOpen; 2015:4.

Drug Design, Development and Therapy

Dovepress

Publish your work in this journal

Drug Design, Development and Therapy is an international, peer-reviewed open-access journal that spans the spectrum of drug design and development through to clinical applications. Clinical outcomes, patient safety, and programs for the development and effective, safe, and sustained use of medicines are a feature of the journal, which has also been accepted for indexing on PubMed Central. The manuscript management system is completely online and includes a very quick and fair peer-review system, which is all easy to use. Visit <http://www.dovepress.com/testimonials.php> to read real quotes from published authors.

Submit your manuscript here: <https://www.dovepress.com/drug-design-development-and-therapy-journal>